Műszaki Tudományos Közlemények vol. 22. (2025) 116–122.
DOI: Hungarian: https://doi.org/10.33895/mtk-2025.22.20
English: https://doi.org/10.33894/mtk-2025.22.20

DESIGN AND FINITE ELEMENT SIMULATION OF ZETOR 10245 TYPE AGRICULTURAL TRACTOR BALANCER AXLE TURNING TECHNOLOGY

Csaba VARGA,[1] Attila SZÁNTÓ,[2] Tamás Gergő ASZTALOS,[3] Szabolcs Sándor DIÓS,[4] Géza HUSI[5]

[1] *Debrecen University, Faculty of Engineering, Department of Vehicles Engineering, Debrecen, Hungary, csabavarga.t@gmail.com*

[2] *Debrecen University, Faculty of Engineering, Department of Basic Technical Studies, Debrecen, Hungary, szanto.attila@eng.unideb.hu*

[3] *Debrecen University, Faculty of Engineering, Hungary, gergoasztalos.28@gmail.com*

[4] *Debrecen University, Faculty of Informatics, Debrecen, Hungary, dios.szabolcs@eng.unideb.hu*

[5] *Debrecen University, Faculty of Engineering, Department of Vehicles Engineering, Debrecen, Hungary, husigeza@eng.unideb.hu*

Abstract

The project is investigating the production of a balancer shaft for the Zetor 10245 tractor, focusing on vibration reduction for in-line four-cylinder engines. Using 100Cr6 high-carbon bearing steel, advanced meg-machining techniques and finite element simulations were applied to optimize performance and life. Stress analysis, toolpath optimization and precision machining on a DMG MORI NT 4250 DCG machine ensured structural integrity and high-quality output. Surface roughness and performance measurements validated the design, demonstrating the effective integration of material selection, machining and simulation to increase engine reliability.

Keywords: *balance shaft, 100Cr6 steel, finite element simulation, machining optimization.*

1. Introduction

The Debrecen region is not only important for the automotive industry, but also for agriculture. That is why, in addition to the low-tech vehicles, tractor-related developments and maintenance are also important.

The balancer axle plays a critical role in reducing vibration in in-line four-cylinder engines by counteracting first- and second-order forces. Using 100Cr6 high-carbon steel, advanced machining processes such as turning, milling and grooving were applied to achieve accuracy and durability. Finite element simulations were carried out to evaluate stress distribution, deformations and performance under realistic conditions. This integrated approach ensures the production of a reliable component that increases the efficiency and lifetime of the motor. The Zetor 10245 tractor is shown in **Figure 1.**

1.1. Analysis of the balancing axis

Several wear patterns were evident at the bearing location, including diameter reduction and ovality due to the geometry of the shaft, and indentations outside the bearing contact surfaces probably occurred after the gear slipped, as the shaft continued to rotate to maintain momentum

Fig. 1. *Zetor 10245 at work in spring.*

from its mass. The shaft itself can be seen in Figure 2.

The various instances of wear all point in the same direction, even when achieving material-side design life in bearing and shaft terms, so the following case was inevitable [1, 2].

1.2. Material choice

The Sauter HO ultrasonic hardness tester was an extremely valuable tool in this project to evaluate the material hardness and surface roughness of the balancer shaft. The measuring instrument used is shown in Figure 3.

The results of the tests showed that it has almost uniform hardness parameters on both sides, except for the bearing surfaces of the component, which exhibit extremely high strength and wear resistance for longer shaft life. The hardness measurement results are summarized in Table 1.

1.3. Selected material

For the balancer shaft, We chose 100Cr6, a steel with excellent strength, toughness and wear resistance, making it an optimal choice for sub-assemblies that are subjected to dynamic loads and stresses during operation (Figure 4).

2. 3D model design

The following measurement tools were used in the design:

- Digital caliper: for measuring the outside diameter, length and distance between critical surfaces of the shaft.
- Stirrup micrometer: used to measure the diameter of the shaft, ensuring a fine tolerance within the Mechani-Kai limits.
- Radius template set: with the help of this tool the curves and the radius on the balancing shaft were measured.

In the initial phase of the 3D modelling process, 2D sketches of the shaft were created in SolidEdge [5].]. Using the data obtained from the measurements, two-dimensional profiles were created for the most important cross-sections, namely the shaft diameter, the gear positions and the grooves for the curved latch nest.

In addition to refining the 3D model, Fusion 360 was used to design and simulate the machining process. The first step in the process is the set-up of the stock, which involves defining the dimensions of the cylindrical stock. A solid bar with a diameter of 55mm and a length of 700mm was used as the basis for the part, and the stock was positioned for the machining operations.

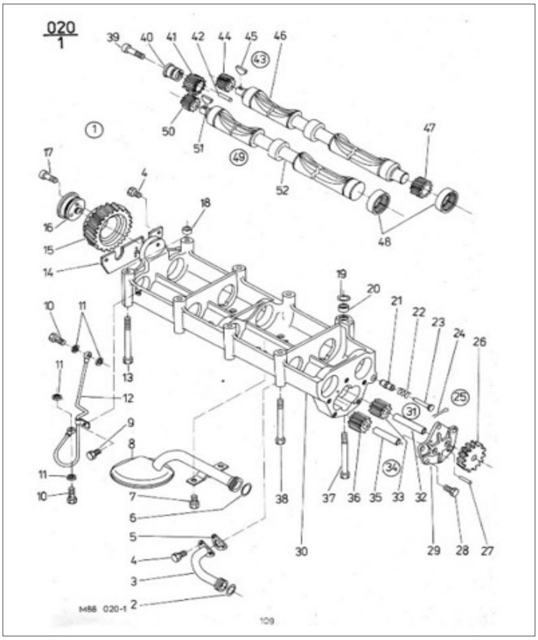

Fig. 2. *Exploded view of the balancing unit.* [3]

Fig. 3. *The Sauter HO hardness tester.*

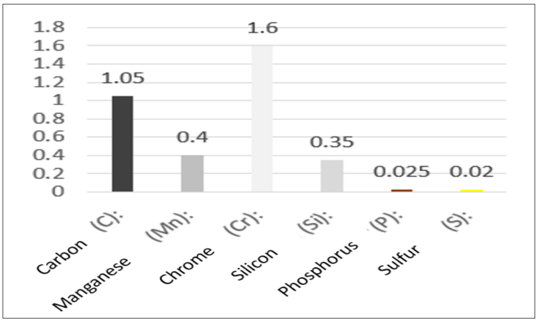

Fig. 4. *Chemical composition diagram of 100Cr6.* [4]

Table 1. *Results of the hardness measurement*

1.	2.	3.	4.	5.	6.	7.
21.6 HRC	56.7 HRC	31.1 HRC	58.9 HRC	30.8 HRC	56.9 HRC	22.1 HRC
22.2 HRC	48.1 HRC	27.9 HRC	55.9 HRC	29.2 HRC	57.7 HRC	28.3 HRC

3. Turning processes

During turning, each operation serves a specific purpose in shaping and machining the workpiece to meet the desired machining properties. In this section, We discuss the characteristics and parameters of each operation, including homo-locating, longitudinal turning roughing, longitudinal turning smoothing, external recess roughing, external recess smoothing, drilling and profile finishing [6]. The imported model is shown in Figure 5.

The tools used in the process, i.e. those recommended by Sandvik Hungary Ltd., were carefully selected to achieve the required accuracy, optimum surface quality and efficient material removal (Figure 6) [7].

To ensure that the end points of the shaft are perfectly flat and accurately dimensioned, face machining was used. During this turning process, the tool is moved radially towards the centre line at the workpiece end.

The values used for the frontal stiffening are summarised in Table 2.

Longitudinal turning, or straight turning, is a machining operation in which the cutting tool moves in a direction parallel to the axis of the rotating workpiece, thereby reducing the diameter in the longitudinal direction. External grooving is a turning operation in which the cutting tool creates a groove or recess along the external diameter of the cylindrical workpiece. In external grooving, the tool is inserted directly into the workpiece at the desired location and moves radially in the material to achieve the desired depth. Chamfering, also important, is a turning operation used to separate the finished part from the rest of the workpiece or bar stock (Figure 7).

In the parting operation, the cutting tool is inserted indirectly into the rotating workpiece until it reaches the centre, effectively cutting through the diameter and creating a separate sub-part.

The catch values are summarised in Table 3.

4. Turning processes

Each process has specific characteristics, applications and operating parameters that affect efficiency, accuracy and surface quality [10]. Milling operations are a type of operation in which a flat-end milling cutter is used to create precise, flat-bottomed pockets and other complex profiles on the workpiece. In the case of a balancing spindle, for example, the pockets are machined to achieve the desired mass distribution, which is essential for vibration reduction and proper op-

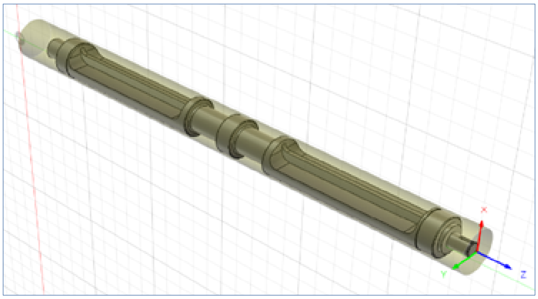

Fig. 5. *Model designed in Fusion 360.*

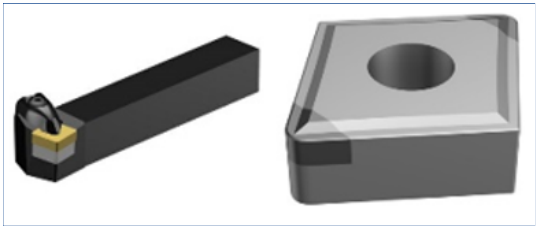

Fig. 6. *DCKNR 2020K 12 turning lathe blade holder and CNGM12041 2F-HGR 7125 blade.* [8, 9]

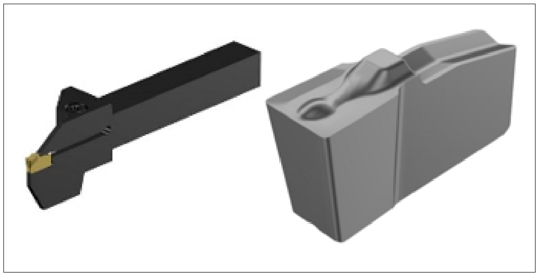

Fig. 7. *RF151.23-08-25 lathe insert holder and 25-4G 525 lathe insert.* [12]

Table 2. *Catches and their characteristics during frontal lobing*

	Roughing	Smoothing
Number of passes	8	1
Cutting speed v_c	145 m/min	145 m/min
Speed feed per revolution f_n	0.177 mm	0.19 mm
Depth of grip a_p	0.567 mm	0.465 mm

Table 3. *Catches and their characteristics during external stabbings*

Number of passes	1
Cutting speed v_c	124 m/min
Speed feed per revolution f_n	0.2 mm
Maximum rotation speed	4000 rpm

Table 4. *Catches and their characteristics during flat-end milling*

Cutting speed v_c	236 m/min
Feed per tooth f_z	0.0901mm
Maximum grip depth	25 mm

Fig. 8. *930-B30-S-20-088 tool holder and 1P330-2000-XA 1620 solid carbide shank grinder for medium roughing.* **[14, 15]**

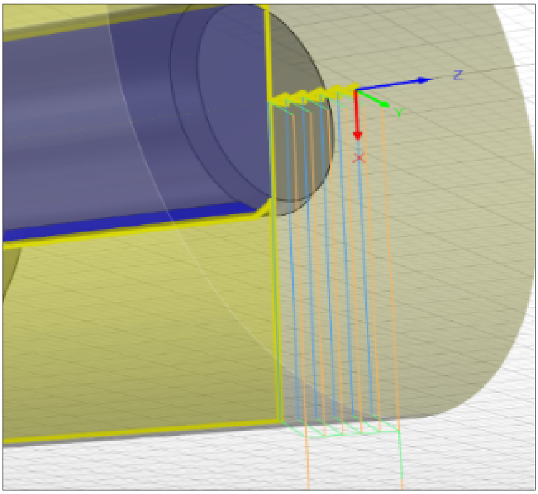

Fig. 9. *Toolpath for the frontal machining process.*

eration **[11]**. The toolholder and the shank milling cutter can be seen in **Figure 8.**

The values for flat-end milling are summarised in **Table 4.**

5. Generating the toolpath

We designed the toolpaths for the machining process using the integrated CAM tools provided by Fusion 360 **[13]** using the different tools we found suitable during my research: depth of cut, cutting speed, radial depth of cut, feed per tooth (**Figure 9**).

For each section of the shaft, specific operations were selected and the corresponding parameters were set, such as main spindle speed, feed per revolution (**Figure 10**).

A series of simulations were carried out to gain insight into how each cutting tool interacts with the material. Ansys was also used to perform the simulations **[16]**.

The simulations showed in real time the manufacturing process from material removal to the final shape of the finished balance shaft (**Figure 11**).

6. Component handling method

When machining the balancer shaft, six-part machining was critical to ensure accuracy and efficiency. The use of primary and secondary spindles ensured safe retention and through-feed of the workpiece during the various machining stages. The main spindle initially held the workpiece, ensuring stability during operations such

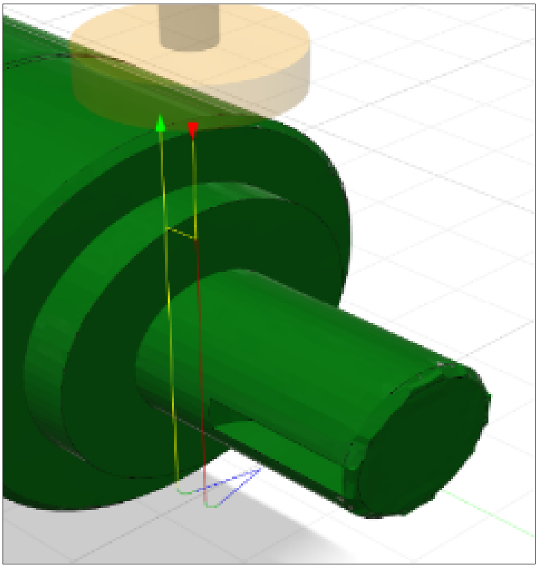

Fig. 10. *Curved bolt grooving, milling process tool path.*

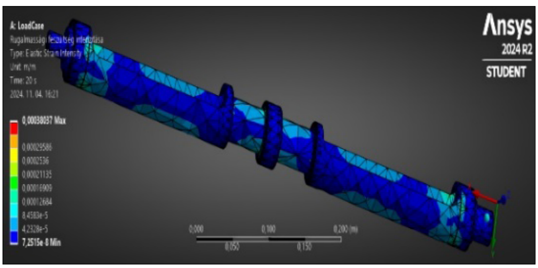

Fig. 11. *Elastic tension intensity test result.*

as longitudinal turning, face turning and grooving (Figure 12).

Once the primary operations were complete, the spindle engaged to hold the opposite end of the spindle, facilitating a smooth transfer of the part without the need for manual repositioning.

7. Finite element simulation

We performed a comprehensive finite element simulation to analyse the performance of the flywheel shaft under different operating conditions. The aim of the simulation was to create a realistic model that accurately represents the physical behaviour of the balancer shaft when subjected to different forces and conditions.

The simulation has highlighted the axial deformation along the length of the shaft due to the axle load and bearing forces. The axial deformation can cause the shaft to elongate slightly under high loads, leading to possible displacement of critical surfaces. Such deflections can lead to uneven load distribution on bearings and coupling components, which can result in increased wear or even mechanical failure [4].

The radial deflection, i.e. the deflection when the axle is subjected to bending stresses, has also been understood, especially in areas subject to geometric deformation, such as grooves or reduced cross-sections.

The application of elastic strain intensity analysis allowed the safe operating parameters of 100Cr6 to be determined, ensuring that the elastic properties of the material are capable of accommodating the expected loading conditions of the tensile field. The deformation values can be seen in Figure 13.

The methods and technologies used in the design and manufacture of the balancer shaft have demonstrated that the combination of appropriate material selection, precision machining and simulation is key to producing reliable and durable components. The use of 100Cr6 material, the state-of-the-art DMG MORI NT 4250 DCG machine and optimised machining parameters contributed to the high quality of the final product. The tests carried out, such as surface roughness and hardness measurements, confirmed that the shaft meets the stringent requirements of agricultural machinery. This project provided an effective solution to increase the reliability and lifetime of the Zetor 10245 tractor.

9. Research infrastructure

The University of Debrecen, Faculty of Technology has implemented a number of improvements in the laboratories, which will be decisive in the coming period. The established automotive lab provides the opportunity to start new developments in the field of robotics [17]. The field of artificial intelligence is gaining significant ground in the industry, therefore we started to complement the basic robot functions in the automotive lab based on our own dataset [18]. For the preliminary teaching we used Digital-Twin techniques in the lab [19]. The automotive engineering lab is also significant for the Faculty of Engineering, as the region is now mainly defined by the automotive industry, so that optimizations [20] and machine learning solutions can open new innovative avenues [21]. Simulations on vehicle dynamics were also performed in the lab, on the topic of electric motors [22], based on previous telemetry data [23]. DAQ data acquisition systems have been used for these [24], which have also been used in our aircraft development [25].

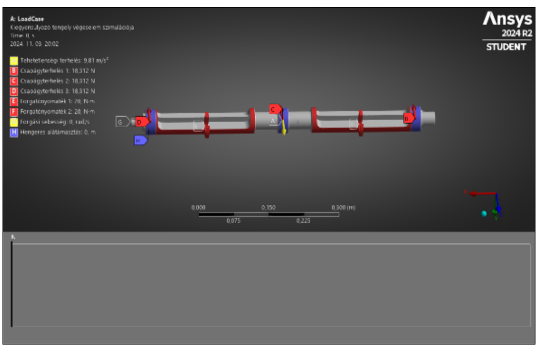

Fig. 12. *Ansys 2024 R2 model created in student-licence software.*

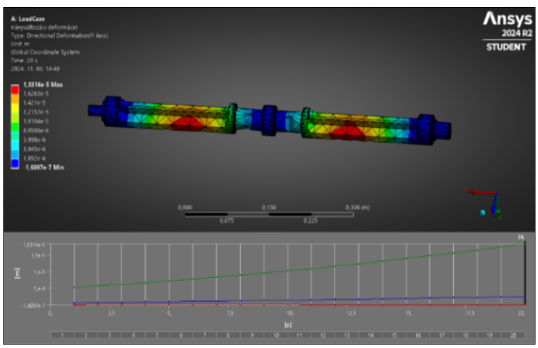

Fig. 13. *Result of the deformation marker test.*

Acknowledgements

We would like to express our sincere gratitude to Timotei Erdei, the head of the Vehicles Engineering Department and the head of the Vehicle Manufacturing Laboratory, and Gábor Balogh, a master's student in mechanical engineering. Also to the University of Debrecen, Faculty of Engineering.

References

[1] *Bearing Damage Evaluation Guide*. SKF Group, Gothen-burg, Sweden, 2017.

[2] *Bearing Damage and Failure Analysis*. SKF Group, Gothenburg, Sweden, 2014.

[3] *Zetor Spare Parts Catalog 8211-16245*. Zetor Tractors a.s., Brno, Czech Republic, Jan. 1990.

[4] 100Cr6, Magas széntartalmú csapágyacél technikai adatlap,inoxservice.hu [Online] https://www.inoxservice.hu/upload/inline/adatlapok/kovacsolttombok/1.3505%20-%20ADATLAP.pdf

[5] Goanta A., Haraga G.: *Aspects of Modelling Classical or Synchronous Modelling with Solid Edge ST. 9*. MATEC Web Conferences, 112. (2017) 06024. https://doi.org/10.1051/matecconf/201711206024

[6] *Handbook of Cutting Data & Parameters – Milling and Drilling*. Ingersoll Werkzeuge GmbH, Haiger, Germany, 2023.

[7] Kalpakjian S., Schmid S. R.: *Manufacturing Engineering and Technology*, 8th ed., Pearson, 2019. https://doi.org/10.1016/B978-0-12-814104-6.00012-3

[8] *Sandvik Coromant Turning Tools*. Sandvik Coromant, Hungary, 2020. p. 206.

[9] *Sandvik Coromant Turning Tools*. Sandvik Coromant, Hungary, 2020. p. 163.

[10] *Sokoldalúan felhasználható tömör keményfém szármarók.* CoroMill Dura [Online] https://www.sandvik.coromant.com/hu-hu/tools/milling-tools-old/solid-carbide-end-mills/coromill-dura/coromill-dura-multimaterial

[11] *Sandvik Coromant Turning Tools*. Sandvik Coromant, Hungary, 2020. p. 409.

[12] *Sandvik Coromant Turning Tools.* Sandvik Coromant, Hungary, 2020. p. 208.

[13] Hassan I., Al-Mashhadi H., Radi K., Jawad H.: *IoT Based Multitasking Games and Entertainment Arcade Station Using Raspberry-Pi*. Journal of Southwest Jiaotong University. 54. https://doi.org/10.35741/issn.0258-2724.54.3.4

[14] Sandvik Coromant Turning Tools, Sandvik Coromant, Hungary, 2020. p. 407.

[15] CoroChuck 930 Nagy pontosságú hidraulikus tokmány, C-1040:266 hu-HU, AB Sandvik Coromant, 2019. p. 2

[16] B. Zheng, J. Zhang, Y. Yao: *Finite Element Analysis of the Piston Based on ANSYS*. IEEE 3rd Information Technology, Networking, Electronic and Automation Control Conference (ITNEC), Chengdu, China, 2019, 1908–1911. https://doi.org/10.1109/ITNEC.2019.8729409

[17] Kapusi T. P., Erdei T. I., Husi G., Hajdu A:. *Application of Deep Learning in the Deployment of an Industrial SCARA Machine for Real-Time Object Detection.* Robotics 11. (2022) 69. https://doi.org/10.3390/robotics11040069

[18] Erdei T. I., Nusser D. P., Husi G.: *Cyber-Physical Recreation of Six DOF Industrial Robot Arm.* International Review of Applied Sciences and Engineering, 15/2. (2024) 147–160. https://doi.org/10.1556/1848.2023.00660

[19] Erdei T. I., Krakó R., Husi G.: *Design of a Digital Twin Training Centre for an Industrial Robot Arm*. Applied Sci.ences, 12/17. (2022) 8862. https://doi.org/10.3390/app12178862

[20] Ahmed M., Sulaiman M. H., Hassan M. M., Rahaman M. A., Abdullah M.: *Selective Opposition Based Constrained Barnacle Mating Optimization: Theory and Applications*. Results in Control and Optimization, 17. (2024) 100487. https://doi.org/10.1016/j.rico.2024.100487

[21] Deshpande A. R., Kulkarni A. P., Wasatkar N., Gajalkar V., Abdullah M.: *Prediction of Wear Rate of Glass-Filled PTFE Composites Based on Machine Learning Approaches*. Polymers, 16/18. (2024) 2666. https://doi.org/10.3390/polym16182666

[22] Szántó A., Ádámkó É., Juhász G., Sziki G. Á.: *Simultaneous Measurement of the Moment of Inertia and Braking Torque of Electric Motors Applying Additional Inertia.* Measurement, 204. (2022) 112135. https://doi.org/10.1016/j.measurement.2022.112135

[23] Sziki G. Á., Szántó A., Kiss J., Juhász G., Ádámkó É.: *Measurement System for the Experimental Study and Testing of Electric Motors at the Faculty of Engineering*. University of Debrecen. Applied Sciences, 12/19. (2022) 10095. https://doi.org/10.3390/app121910095

[24] Dave G. S., Pandhare A. P., Kulkarni A. P., Khanka, D. V., Abdullah M.: *Experimental Investigation of Centrifugal Pump Machine and Its Faults through Different Type of DAQ System and Selecting One Based on Statistical Approach*. Cogent Engineering, 11/1. (2024). https://doi.org/10.1080/23311916.2024.2417683

[25] Abdullah M., Husi G.: *Aero Graphene in Modern Aircraft & UAV*. Recent Innovations in Mechatronics, 9/1. (2022).
https://doi.org/10.17667/riim.2022.1/4